Phase Angle Control of Three Level Inverter Based D-STATCOM Using Neuro-Fuzzy Controller

Resul COTELI[1], Erkan DENIZ[1], Besir DANDIL[1], Servet TUNCER[2], Fikret ATA[3]
[1]*University of Firat, Technical Education Faculty, Electrical Science, Elazig, 23119, Turkey*
[2]*Technical Education Faculty, Electronic and Computer Science,Elazig, 23119,Turkey*
[3]*University of Firat, Electrical and Electronics Engineering,Elazig, 23119,Turkey*
rcoteli@firat.edu.tr

***Abstract*—Distribution Static Compensator (D-STATCOM) is a shunt compensation device used to improve electric power quality in distribution systems. It is well-known that D-STATCOM is a nonlinear, semi-defined and time-varying system. Therefore, control of D-STATCOM by the conventional control techniques is very difficult task. In this paper, the control of D-STATCOM is carried out by the neuro-fuzzy controller (NFC) which has non-linear and robust structure. For this aim, an experimental setup based on three-level H-bridge inverter is constructed. Phase angle control method is used for control of D-STATCOM's output reactive power. Control algorithm for this experimental setup is prepared in MATLAB/Simulink and downloaded to DS1103 controller card. A Mamdani type NFC is designed for control of D-STATCOM's reactive current. Output of NFC is integrated to increase tracking performance of controller in steady state. The performance of D-STATCOM is experimentally evaluated by changing reference reactive current as on-line. The experimental results show that the proposed controller gives very satisfactory performance under different loading conditions.**

***Index Terms*—electric power quality, D-STATCOM, three-level H-bridge inverter, neuro-fuzzy controller, MATLAB.**

I. INTRODUCTION

Recently, electrical power quality problems have been increased as a result of widespread use of power semiconductor components. There are many methods for the solution of the power quality problems in distribution systems such as using surge arresters, active power filters, isolation transformers, uninterruptible power supplies and static VAR compensators [1]. The inverter based custom power devices have been widely used in many utilities because of their fast response and good steady state performance over conventional compensators [2]. The D-STATCOM is an inverter based custom power device used for the voltage regulation, power factor correction and load balancing.

Control method has a vital important over the whole performance of the D-STATCOM [3]. The system are controlled to obtain desired performance depending on the operational requirements, type of applications, system configuration and loss optimisation [3]. The control method to be preferred for D-STATCOM is simple its algorithm and easy to implement [4]. Different control methods such as phase angle control, direct current control, indirect current control and constant dc-link voltage scheme are proposed for dynamic control of D-STATCOM's output reactive power [5, 6]. Phase angle control method has advantages such as its simple algorithm and easy to perform [2].

Conventionally, phase angle control method is carried out by Proportional Integral (PI) controller designed according to linear control techniques. In this control method, position of characteristic roots on the complex plane is depended on phase angle. To design a controller based on linear control methods for phase angle controlled D-STATCOM, equations are linearized for specific operating point by some assumptions. Nevertheless, it is impossible to free the position of characteristic roots from phase angle in real-time applications. In addition, such controllers may not give the desired performance due to parameter variation, load disturbance, unmodelled dynamics of the plant [7, 8].

To cope with disadvantages of linear control methods, some researchers suggested non-linear control methods such as H_∞, differential algebra theory, exact linearization with feedback [8-12]. Such control methods need exact mathematical model and parameters of controlled system. Besides, controller design with these methods has a more complex structure and is more difficult to realize than linear controllers [8].

To obtain a good performance both in transient and steady state from D-STATCOM, controller should be nonlinear and robust structure and independent from mathematical model of controlled system. Recently, intelligent controllers as alternative linear and nonlinear control techniques have been used in the control of D-STATCOM [13-18]. In case of using the intelligent controllers, there is no need the mathematical model of the controlled system. Moreover, such controllers can provide efficient control over wide operating conditions which distinguishes them from conventional linear controllers [8]. NFC is an intelligent controller that is based on Fuzzy Logic Controller (FLC) whose functions are realized by Artificial Neural Network (ANN) and it has been successfully applied to the most of control problems. NFCs are substantially effective in control of nonlinear systems [19]. In [20], NFC is used for current control of D-STATCOM using indirect current control method. But, experimental results with this kind of control method haven't been reported previously for D-STATCOM in literature.

This work was supported by Scientific and Technology Research Council of Turkey (TUBITAK) with 107E245 numbered project.

Digital Object Identifier 10.4316/AECE.2012.01013

In this paper, the robust nonlinear control strategy based NFC with fuzzy singleton rules is proposed for phase angle control of D-STATCOM to achieve a good dynamic response under the all possible loading conditions. Designed NFC has two inputs, single output and four layers. Inputs of NFC are chosen as error of q-axis current and variation of this error. An anti wind-up integrator is used to improve tracking capability of NFC in steady state. The gradient descent algorithm is used to train the NFC in direct adaptive control scheme using the simulation model of the D-STATCOM and then trained NFC is used in experimental study. This paper is organized as follows. In Section 2, operation principle of D-STATCOM is summarized. Power circuit and mathematical model of three-level H-bridge inverter based D-STATCOM is given in Section 3. The description of the NFC and its training algorithm are explained in Section 4. The experimental results related to proposed controller are given in Section 5. Section 6 provides conclusions of this study

II. Basic Operation Principle of D-Statcom

The basic operation principle of D-STATCOM can be explained by Fig. 1. From this figure, D-STATCOM is connected to Bus2. The amount of the reactive power flowing from Bus1 to Bus2 mainly depends on the voltage difference between both buses. Reactive power flows from the higher voltage to low voltage. In the phase angle control method, the amplitude of inverter output voltage is controlled by causing a small amount of active power flow into/out of the D-STATCOM. If V_i lags V_s, a small amount of active power flows into D-STATCOM and dc-link capacitor voltage increases by charged. On the contrary, a small amount of active power flows out D-STATCOM, thus the dc-link capacitor voltage decrease by discharged. Briefly, dc-link voltage is controlled by adjusting phase angle δ between the V_s and V_i voltages.

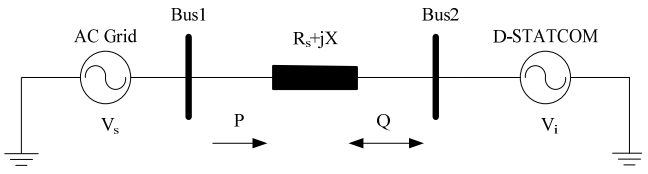

Figure 1. Simple two-bus system in which D-STATCOM is connected

The amount of active power flow between D-STATCOM and ac grid is expressed as Eq.(1).

$$P = \frac{V_s V_i}{X} \sin \delta \tag{1}$$

The large amount of reactive power generated/absorbed by the D-STATCOM can be also controlled by flowing the small amount of active power. The amount of reactive power generated/absorbed by D-STATCOM is also given in (2);

$$Q = \frac{V_s}{X}(V_s - V_i \cos \delta) \tag{2}$$

III. Three-Level Inverter Based D-Statcom

Inverters are convetionally controlled as a PWM voltage source in medium and high-power applications because of switching losess. Since the converter is operated as a PWM voltage source, the switching frequency of the devices can be properly controlled. However, harmonic distortion in the generated reactive current is much more than that of a controlled current scheme. To reduce low-order harmonics, either inverter have been operated in parallel or multilevel converters should be used. In a inverter structure operated in parallel, the input transformer becomes bulky [21]. Recently, multilevel inverters have been widely used in fast controllable reactive power applications. These inverter topologies used in reactive power applications offer considerable advantages over parallel converter operations in terms of space reductions, cost and losess. Cascaded inverter is the most popular topology among multilevel inverters because of using minimum number of components and its modular structure [22]. The number of lowest voltage-level in the cascaded inverters is three. In addition, dc voltage unbalance doesn't occurred in three-level. In this study, three-level H-bridge inverter is preffered for power circuit of D-STATCOM. Flexible structure of this inverter easily allows to increase the number of voltage-level by adding the H-bridges in series to per phase.

Power circuit of three-level H-bridge inverter based D-STATCOM is illustrated in Fig. 2. D-STATCOM consists of three H-bridge inverters, three dc-link capacitors (C) supplying the dc voltages to H-bridge inverters and a coupling inductance with internal resistance ($\omega L_s + R_s$) connecting to ac grid the inverter.

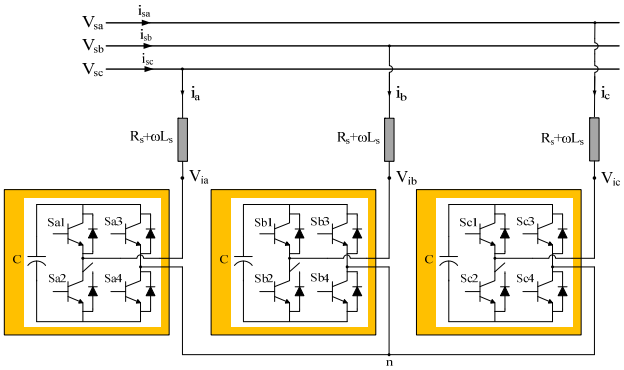

Figure 2. Power circuit of three-level H-bridge inverter based D-STATCOM

Mathematical model of H-bridge inverter based D-STATCOM can be derived from Fig. 1. The circuit equation on stationary reference frame can be written as follows,

$$L_s \frac{d\underline{i}}{dt} + R_s \underline{i} = \underline{V}_s - \underline{V}_i \tag{3}$$

The $\underline{V}_s$ is defined as complex voltage vector of grid and the $\underline{V}_i$ is also defined as complex voltage vector of inverter. Space vector theory based on synchronous reference frame is applied to D-STATCOM. Coordination of vector space is shown in Fig. 3. The αβ and dq-axes represent stationary reference and synchronous rotating frame, respectively. Voltage vectors and current vector in complex plane are expressed in stationary reference frame as follows [23];

$$\underline{V}_s = V_{sa} + V_{sb}e^{j\gamma} + V_{sc}e^{2j\gamma} = V_s e^{j\lambda} \quad (4)$$

$$\underline{V}_i = V_{ia} + V_{ib}e^{j\gamma} + V_{ic}e^{2j\gamma} = V_i e^{j(\lambda-\delta)} \quad (5)$$

$$\underline{i} = i_a + i_b e^{j\gamma} + i_c e^{2j\gamma} = ie^{j(\varphi+\lambda)} \quad (6)$$

Where, $\gamma = 2\pi/3$, V_{sabc} and V_{iabc} are instantaneous phase voltages of grid and D-STATCOM, respectively. The d-axis of the space vector diagram shown in Fig. 3 is assigned to coincide with the V_i. Complex vectors in the stationary reference frame are transformed onto synchronous rotating frame by multiplying them with unity space vector $e^{-j\lambda}$ as follows [23];

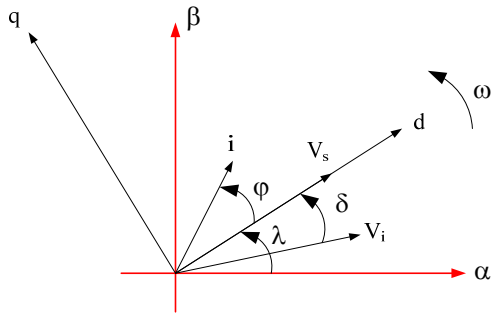

Figure 3. Coordinate system for synchronous rotating reference frame

$$L_s e^{-j\lambda}\frac{d\underline{i}}{dt} + R_s e^{-j\lambda}\underline{i} = \underline{V}_s e^{-j\lambda} - \underline{V}_i e^{-j\lambda} \quad (7)$$

$$\underline{V}_s e^{-j\lambda} = v_{sd} + jv_{sq} \quad (8)$$

$$\underline{V}_i e^{-j\lambda} = v_{id} + jv_{iq} = v_i\cos\delta - jv_i\sin\delta \quad (9)$$

$$\underline{i}\, e^{-j\lambda} = i_d + j\, i_q \quad (10)$$

By substituting (7), (8), (9) into (10), the circuit equations in dq-axis are obtained as (11) and (12).

$$L_s\frac{di_d}{dt} + R_s i_d = v_{sd} - v_i\cos\delta + L_s\omega i_q \quad (11)$$

$$L_s\frac{di_q}{dt} + R_s i_q = v_{sq} - v_i\sin\delta - L_s\omega i_d \quad (12)$$

Where, ω is frequency of grid. Peak value of inverter output voltage is expressed as (13).

$$V = M_a V_{dc} \quad (13)$$

In (13), M_a is modulation index and V_{dc} is dc-link voltage. From instantaneous power equality on the dc side and the ac side of the inverter, power equation can be written as (by neglecting the system losses) [24];

$$P_c = V_{dc}I_{dc} = \frac{3}{2}(v_{id}I_d + v_{iq}I_q) \quad (14)$$

Where I_{dc} is the capacitor current. Capacitor current is also descibed as follows,

$$I_{dc} = \frac{3}{2}M_a(i_d\cos\delta + i_q\sin\delta) = C\frac{dV_{dc}}{dt} \quad (15)$$

State equations for ac side of three-level H-bridge inverter based D-STATCOM are given by (11) and (12) whereas Eq.(15) presents state equation for dc side of three-level H-bridge inverter based D-STATCOM. ac and dc side circuit equations in dq-axis can be rearranged in state space matrix form as (16). It is shown that circuit equations of D-STATCOM are nonlinear if δ is taken as input variable. The circuit equations should be linearized around the certain operation point for controller design based on linear control method. Assuming that V_{sd} and V_{sq} are constant value, linearization of Eq.(16) around the operation point δ_0 presents a set of linear equations given in (17) [23].

$$\frac{d}{dt}\begin{bmatrix} i_d \\ i_q \\ V_{dc} \end{bmatrix} = \begin{bmatrix} -R_s/L_s & \omega & -M_a\cos\delta/L_s \\ -\omega & -R_s/L_s & M_a\sin\delta/L_s \\ \dfrac{3M_a\cos\delta}{2C} & -\dfrac{3M_a\sin\delta}{2C} & 0 \end{bmatrix} \times \begin{bmatrix} i_d \\ i_q \\ V_{dc} \end{bmatrix} + \begin{bmatrix} 1/L_s & 0 \\ 0 & 1/L_s \\ 0 & 0 \end{bmatrix} \times \begin{bmatrix} v_{sd} \\ v_{sq} \end{bmatrix} \quad (16)$$

$$\frac{d}{dt}\begin{bmatrix} i_d \\ i_q \\ V_{dc} \end{bmatrix} = \begin{bmatrix} -R_s/L_s & \omega & -M_a\cos\delta_0/L_s \\ -\omega & -R_s/L_s & M_a\sin\delta_0/L_s \\ \dfrac{3M_a\cos\delta_0}{2C} & -\dfrac{3M_a\sin\delta_0}{2C} & 0 \end{bmatrix} \times \begin{bmatrix} i_d \\ i_q \\ V_{dc} \end{bmatrix} + \begin{bmatrix} (\dfrac{M_a}{L_s}V_{dc0}\sin\delta_0)\delta \\ (\dfrac{M_a}{L_s}V_{dc0}\cos\delta_0)\delta \\ -\dfrac{3M_a}{2C}(i_{d0}\sin\delta_0 + i_{q0}\cos\delta_0)\delta \end{bmatrix} \quad (17)$$

The characteristic equation of system given by (17) is expressed by (18).

$$s^3 + 2\frac{R_s}{L_s}s^2 + \left\{\left(\frac{R_s}{L_s}\right)^2 + \frac{3M_a{}^2}{2L_sC} + \omega^2\right\}s + \frac{3M_a{}^2R_s}{2L_s{}^2C} \quad (18)$$

IV. Structure of Neuro-Fuzzy Controller

FLC is able to make inferences from an expert knowledge. ANN has features such as learning, generalization and adaptation. NFC is an intelligent control method combining the features of FLC and ANN. Basically, NFC is based on the principle which the functions of FLC are implemented by ANN [25]. Therefore, NFC shows features of a nonlinear controller that has abilities such as

learning, adaptation and making inferences. In addition, NFC doesn't need mathematical model of the system to be controlled. Mentioned features make NFC superior when compared with other controllers.

In this study, parameter learning of NFC with fuzzy logic rules whose consequents are fuzzy singleton and its network architechture are shown in Fig. 4. Fuzzy singleton rules are in the following form.

$$R^j: \text{IF } x_1 \text{ is } A_1^j \text{ AND } x_2 \text{ is } A_2^j \text{ THEN y is } w_j \qquad (19)$$

Where, x_i is an input variable, y is output variable, A_i^j is linguistic terms of precondition part with membership function $\mu_{A_i^j}(x_i)$, w_j is real number of the consequent part, j=1, 2, …M and i=1, 2, ..n.

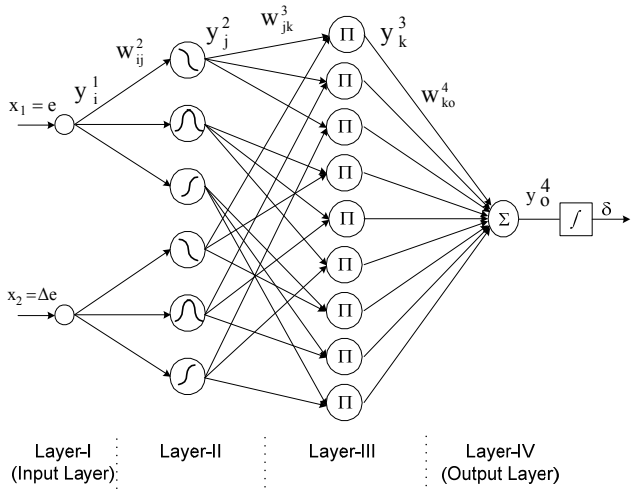

Figure 4. Architecture of NFC

As shown in Fig.4, the NFC consists of four layers. In Layer-I, the input variables of NFC are presented and they are given by (20) and (21).

$$e(k) = i_{qref}(k) - i_q(k) \qquad (20)$$

$$\Delta e(k) = e(k) - e(k-1) \qquad (21)$$

Where, e, i_{qref} - i_q, is the current tracking error and Δe is variation of current error. , i_{qref} and i_q are also the reference and actual currents for q-axis, respectively.

The Layer-II calculates the degree of membership functions for the input values. The Gaussian activation function are utilized to represent the membership functions. The weights between the input and membership layers are assumed to unity. The output of this layer is expressed as;

$$net_j^2 = -\frac{(x_i - m_{ij})^2}{2(\sigma_{ij})^2}, \quad y_j^2 = \exp(net_j^2) \qquad (22)$$

Where, σ_{ij} and m_{ij} are the standard deviation and mean of the Gaussian function in the j*th* term of the i*th* input node.

The Layer-III of the NFC includes the fuzzy rule base and the nodes in this layer represented by Π determine the fuzzy rules. Each node takes two inputs, one from the membership value for the current error, and the other from the membership value for the change in current error. For the k*th* rule node;

$$net_k^3 = \prod_j w_{jk}^3 x_j^3 \ , \ y_k^3 = net_k^3 \qquad (23)$$

Where, x_j^3 represents the j*th* input to the node of rule layer, and w_{jk}^3 is assumed to be unity. The output layer acts a defuzifier. The single node in this layer collects all incoming signals from the rule layer to obtain the final results.

$$net_o^4 = \sum_k w_{ko}^4 y_k^3 \qquad (24)$$

Where, the links weights w_{ko}^4 represent the output action of the k*th* rule. The output of the system using the central defuzzification for the Mamdani fuzzy model is given as;

$$y_o^4 = \frac{net_o^4}{\sum_k y_k^3} \qquad (25)$$

Steady state error in the output of NFC is eliminated by using external compensator [20]. Thus, the desired phase angle is obtained from integrated outputs of controller.

The NFC can adjust the fuzzy control rules by modifying the output weights. The parameters of the membership functions and the output weights of NFC are modified using the back-propagation algorithm to minimize the performance index E [26];

$$E = 0.5.e^2 \qquad (26)$$

The parameters w_{ko} in Eq.(24) can be modified as follows [27].

$$w_{ko} = w_{ko} - \eta \frac{\partial E}{\partial w_{ko}} \qquad (27)$$

Where, the *η is* the learning rate. The gradient of the performance index can be derived as follows.

$$\frac{\partial E}{\partial w_{ko}} = -e.\text{sgn}\left(\frac{\Delta i_q}{\Delta y_o^4}\right)\frac{\partial y_o^4}{\partial net_o^4}\frac{\partial net_o^4}{\partial w_{ko}} = \delta \frac{y_k^3}{\sum_k y_k^3} \qquad (28)$$

Where, $\partial i_q / \partial y_o^4$ can be calculated using the dynamics of D-STATCOM. Gradient of the performance index for the parameters of the membership functions can be also derived as (29) and (30).

$$\frac{\partial E}{\partial m_{ij}} = -e.\text{sgn}\left(\frac{\Delta i_q}{\Delta y_o^4}\right)\frac{1}{\sum_k y_k^3} w_{ko}^4 \frac{x_i - m_{ij}}{(\sigma_{ij})^2} y_j^2 \qquad (29)$$

$$\frac{\partial E}{\partial \sigma_{ij}} = -e.\text{sgn}\left(\frac{\Delta i_q}{\Delta y_o^4}\right)\frac{1}{\sum_k y_k^3} w_{ko}^4 \frac{(x_i - m_{ij})^2}{(\sigma_{ij})^3} y_j^2 \qquad (30)$$

IV. Control Strategy of Three-Level Inverter Based D-Statcom

In phase angle control method, modulation index is kept constant and the fundamental voltage component of inverter

is controlled by dc-link voltage. The control variable is therefore δ. In order to change the amount of reactive power delivered/absorbed by D-STATCOM, dc-link voltage should be adjusted by control of δ [28]. Fig. 5 shows phase angle control diagram of D-STATCOM in which phase angle is controlled by NFC. A Software Phase Locked Loop (SPLL) is used to synchronize inverter output voltage with ac grid. Sensed currents and voltages in point of common coupling (PCC) are transformed to dq- axis compenents by using grid frequency obtained from SPLL. The reactive current error and variation of this error are applied to NFC. The integrated output of NFC is reference signal representing δ. Thus, phase angle of modulation signals are obtained. Amplitude of modulation signals M_a is kept constant. Thus, modulation signals for phase-abc are obtained as $M_a\sin(\theta+\delta)$, $M_a\sin(\theta+\delta-2\pi/3)$ and $M_a\sin(\theta+\delta+2\pi/3)$, respectively. Then, PWM signals are produced by three level *Sinusoidal Pulse Width Modulation* (SPWM) technique. In three-level SPWM, two carriers with same frequency and amplitude are used. The reference waveform is centered in the middle of the carrier set and it is continuously compared with each of the carrier signals. If the reference is greater than carrier signal, then the active device corresponding to that carrier is switched on. Otherwise, the active device corresponding to that carrier is switched off.

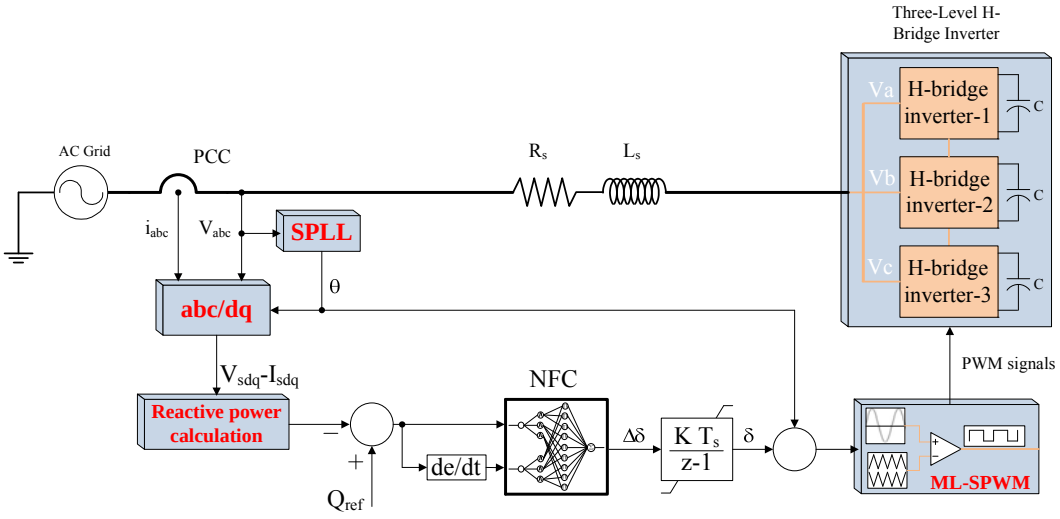

Figure 5. Phase angle control diagram with NFC for D-STATCOM

V. Experimental Results

A DSP-based experimental setup of 8.5kVA is built to validate the operation of the D-STATCOM using NFC. The laboratory setup is shown in Fig. 6. The system can be divided into four parts as power circuit, controller card, measurement&protection circuits and gate drive circuits. A personal computer is used to program the required control algoritm and load the control algorithm to the DS1103 controller card. Three-level H-bridge inverter is constructed by PM75CLA120 IPM modules. This inverter is connected to ac grid via a coupling inductance with internal resistance. A blanking circuit is used to prevent short circuit of switches on the same leg. The current and voltage signals of point of common coupling are sensed by using Hall effect LEM tranducers (LA25-SP1 and LV1000), respectively. During the real-time operation, the sensed current and voltage signals are processed by using the proposed control algorithm and produced PWM signals are applied to the gate drive board. The circuit parameters related to operating condition of D-STATCOM are given in Table I.

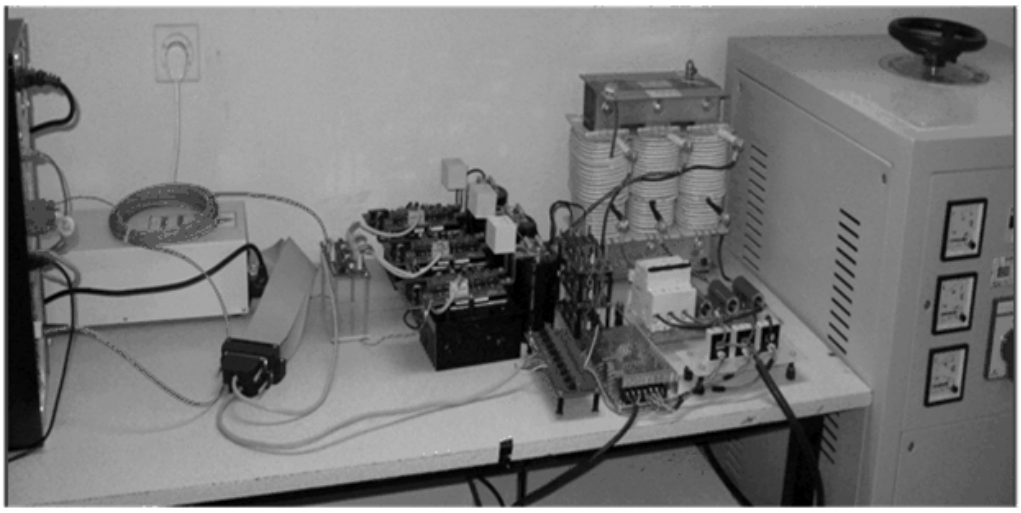

Figure 6. Experimental setup of D-STATCOM

TABLE I. CIRCUIT PARAMETERS RELATED TO OPERATING CONDITION OF EXPERIMENTAL SETUP

Phase voltage of grid	: 200V
Coupling reactance	: 0.1 Ω +j2.89mH
dc-link capacitors	: 3.3mF/450V
Switching frequency	: 1.25kHz
Dead time for each switch	: 4.5μs
Sampling time	: 100μs

A three-phase variac is inserted between the coupling inductance and the ac grid. Before start-up, the output voltage of the variac is adjusted to phase voltage of 200V to charge the dc capacitors. In addition, a resistor is connected in series with the dc capacitors to limit the charging current and then they are bypassed after initial charging. Inverter is controlled by ML-SPWM using fixed switching frequency of 1.25kHz. Laboratory tests of the prototype D-STATCOM are performed to verify the validity of proposed NFC controller. Fig. 7 shows the experimental waveform related to voltages of three dc-link capacitors when the D-STATCOM is started in stand-by mode. From the figure, three dc-link capacitors are firstly charged to about 245V in phase voltage of 200V. Voltages of three dc-link capacitors increase up to 310V after gating signals are applied to switches of inverter. In addition, three dc-link voltage are balanced.

The task of the D-STATCOM is mainly to provide the reactive current for load compensation and voltage regulation and suppress current harmonics. In this study, D-STATCOM is operated in reactive current source mode. For testing of D-STATCOM, a step command for reference reactive current is used to emulate sudden load or voltage changing in system. This case is the worst operating condition for D-STATCOM. During test, reactive current and voltages of three dc-link capacitors are observed. For reactive current and three dc-link capacitors voltages, performance of D-STATCOM is evaluated for settling time, reference tracking and steady state error.

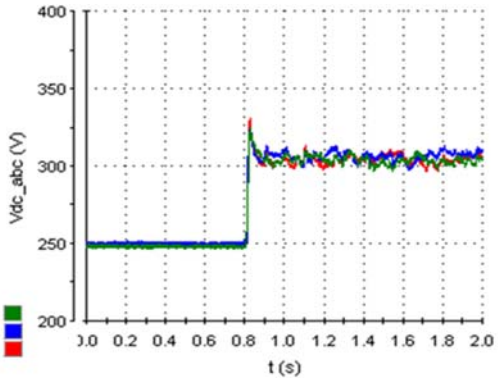

Figure 7. The variations in voltages of three dc-link capacitors when D-STATCOM was put into operation

Figure 8(a) and (b) show the reactive current response of D-STATCOM to step changes in the reactive current command from positive to negative and for opposite direction, respectively. To provide clear view, Fig. 8(a1) and (b1) are also zoomed as shown in Fig. 8(a2) and (b2). It can be seen that D-STATCOM generates/absorbs the reference reactive current in a small period of time for two reference changing. In addition, there is no steady state error in reactive current.

Figure 9(a) and (b) show the changing of three dc-link voltages for same command changes in the reactive current command. It is clearly seen that three dc-link voltages have small overshoots and reach their reference value quickly. In addition, dc-link voltages increase up 350V for capacitive operation mode of D-STATCOM whereas dc-link voltages decrease about 270V for inductive operation mode of D-STATCOM.

The phase-a voltage and current of D-STATCOM are given in Fig. 10(a) and (b) as per-unit (pu). Phase-a current of D-STATCOM is leading about 90° respect to its voltage for capacitive mode. Otherwise, phase-a current of D-STATCOM is laging about 90° respect to its voltage for inductive mode.

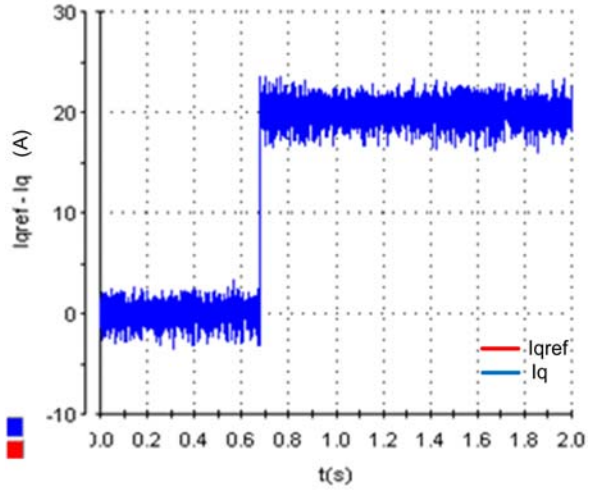

(a1)

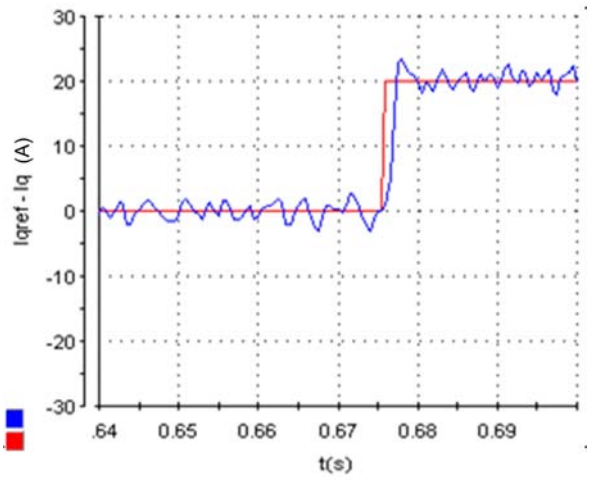

(a2)

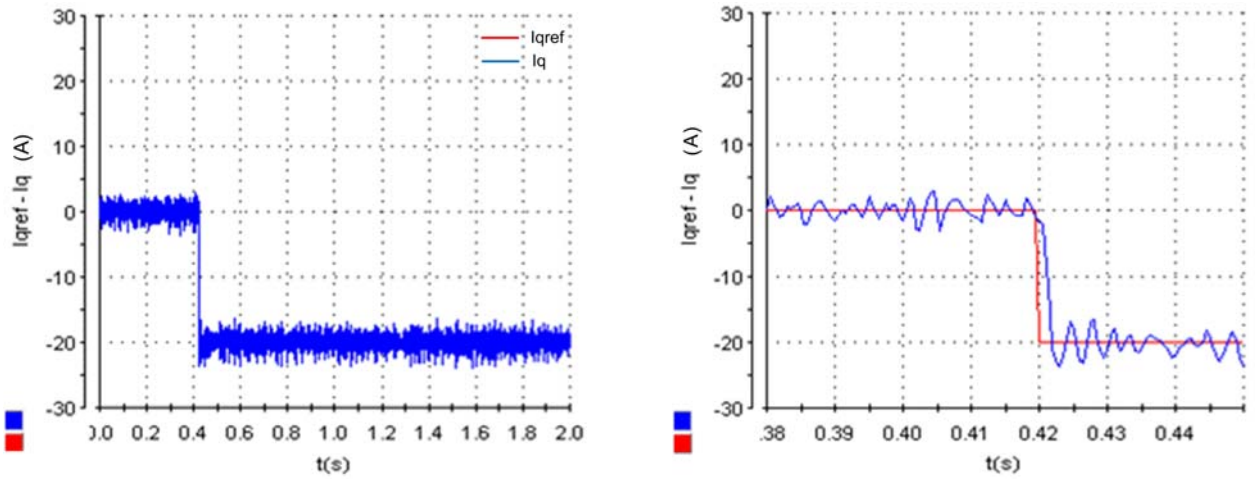

(b1) (b2)

Figure 8. Reactive current response of D-STATCOM, (a) for changing of i_{qref} 0A to +20A, (b) for changing of i_{qref} 0A to -20A

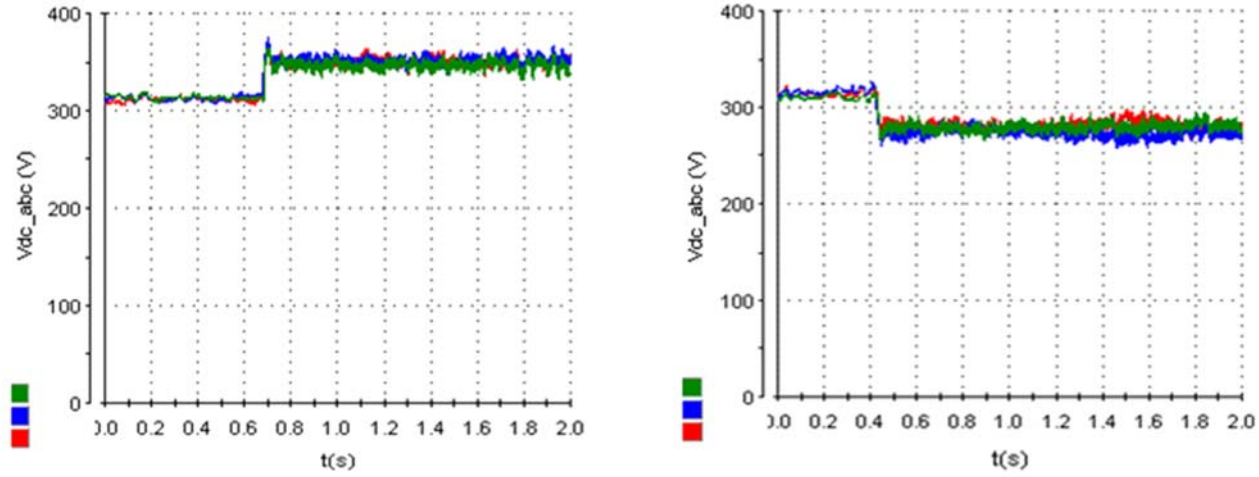

(a) (b)

Figure 9. The variations in voltages of three dc-link capacitors for changing of reference reactive current, (a) 0A to+20A, (b) 0A to -20A

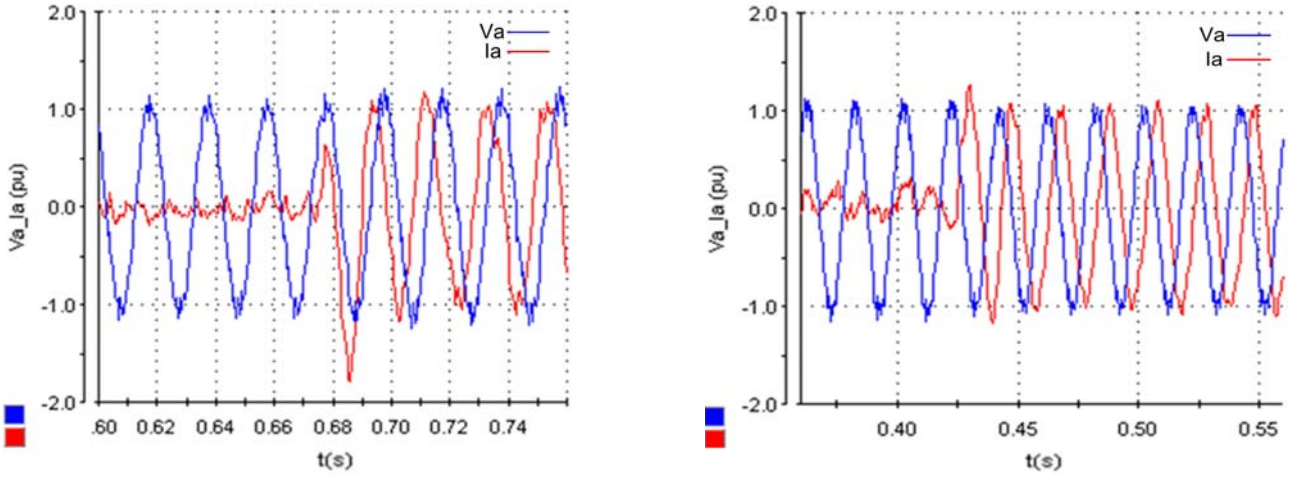

(a) (b)

Figure 10. Relation between phase-a current and voltage for a step change of reference reactive current, (a) 0A to +20A, (b) 0A to -20A

VI. CONCLUSION

In this paper, the application of phase angle controlled D-STATCOM using neural fuzzy networks with singleton rules is presented. The NFC is preffered due to its non-linear and robust structure. In addition, output of NFC is integrated to improve tracking capability in steady state error. Thus, a good control performance is obtained from D-STATCOM both in transient and steady state conditions. The validaty of the proposed control system is shown experimentally for changes of reactive power demand. From the experimental results, very quick response time and accurate compensation effect are obtained by using the proposed control method with NFC.

VII. REFERENCES

[1] H. Masdi, N. Mariun, S. M. Bashi, A. Mohamed and S. Yusuf, "Construction of a Prototype D-STATCOM for Voltage Sag Mitigation", *European Journal of Scientific Research'*, vol. 30, no. 1, pp.112-127, 2009.

[2] D. Masand, S. Jain and G. Agnihotri, "Control Algorithms for Distribution Static Compensator", *Industrial Electronics IEEE International Symposium*, 2006, pp. 1830-1834.

[3] B. Singh, R. Saha, A. Chandra, and K. Al-Haddad, "Static Synchronous Compensators (STATCOM): A Review", *IET Power Electronics*, vol. 2, pp. 297-324, 2009.

[4] B. Singh and J. Solanki, "An Improved Control Approach for DSTATCOM with Distorted and Unbalanced AC Mains", *Journal of Power Electronics*, vol. 8, no. 2, pp.131-140, 2008.

[5] A. Cetin, "Design and Implementation of a Voltage Source Converter Based STATCOM for Reactive Power Compensation and Harmonic Filtering", PhD. Thesis, *The Graduate School of Natural and Applied Sciences of METU*, Ankara, 2007.

[6] S. Kumar, "Static Synchronous Compensators at Distribution and Transmission Levels", *Lecture Note*, 2003.

[7] S. H. Hosseini, R. Rahnavard and Y. Ebrahimi, "Reactive Power Compensation in Distribution Networks with STATCOM by Fuzzy Logic Theory Application", *Power Electronics and Motion Control Conference*, 2006, pp.1-5.

[8] S. Mohagheghi, "Adaptive Critic Designs Based Neuro-controllers for Local and Wide Area Control of a Multimachine Power System with a Static Compensator", PhD Thesis, *Georgia Institute of Technology*, 2006.

[9] F. Liu, S. Mei, Q. Lu, Y. Ni, F.F Wu and A. Yokoyama, A., "The Nonlinear Internal Control of STATCOM: Theory and Application", *International Journal of Electrical Power & Energy Systems*, vol. 25, pp. 421 – 430, 2003.

[10] P. Petitclair, S. Bacha and J. P. Rognon, "Averaged Modelling and Nonlinear Control of an Advanced Static Var Compensator", *Proceedings of the Power Electronics Specialists Conference*, 1996, pp. 753-*758*.

[11] Z. Yao, P. Kesimpar, V. Donescu, N. Uchevin and V. Rajagopalan, "Nonlinear Control for STATCOM Based on Differential Algebra", *29th Annual IEEE Power Electronics Conference*, 1998, pp. 329-334.

[12] X. Yang, H. Hao and Y. Zhong, "The State-Space Modeling and Nonlinear Control Strategies of Multilevel DSTATCOM", *Power and Energy Engineering Conference (APPEEC)*, 2010, pp. 1 – 4.

[13] M. P. Kazmierkowski and L. Malesani, "Current Control Technique for Three-Phase Voltage Source PWM Converters", *IEEE Trans. Ind. Electron.*, vol. 45, no. 5, pp. 691–703, 1998.

[14] L. Malesani and P. Tomasin, "PWM Current Control Techniques of Voltage Source Converters–A Survey", *Int. Conf. Proc. Industrial Electronics, Control and Instrumentation, IECON'93*, 1993, pp. 670–675.

[15] C. Li, Q. Jiang, X. Xie and Z. Wang, "Rule-Based Control for STATCOM to Increase Power System Stability", *Proc.Int. Conf. Power System Technology, POWERCON*, 1998, pp. 372–376.

[16] C. Li, Q. Jiang, Z. Wang and,D. Retzmann, "Design of A Rule-Based Controller for STATCOM", *Proc. Industrial Electronics Society*, 1998, pp. 467–472.

[17] W. Chen, Y. Liu, J. Chen and J. Wu, "Control of Advanced Static VAR Generator by Using Recurrent Neural Networks", *Proc. Power System Technology, POWERCON'98*, 1998, pp. 839–842.

[18] M. Mohaddes, A. M. Gole and P. G. Mclaren, "A Neural Network Controlled Optimal Pulse-Width Modulated STATCOM", *IEEE Trans. Power Deliv.*, vol. 14, no. 2, pp. 481–488, 1999.

[19] B. Dandil, "Fuzzy Neural Network IP Controller For Robust Position Control of Induction Motor Drive", *Expert Systems with Applications*, vol. 36, pp. 528-4534, 2009.

[20] E. Deniz, R. Coteli, B. Dandil, S. Tuncer, F. Ata and M. T. Gencoglu, "Neuro-Fuzzy Current Controller for Three-Level Cascade Inverter Based D-STATCOM", *UPEC'2010: 45th International Universities' Power Engineering Conference,* Cardiff, 31st August- 3rd September 2010, pp. 1-5.

[21] K. Chatterjee, D. V. Ghodke, A. Chandra and K. Al-Haddad, "Simple Controller for STATCOM-Based Var Generators", *IET Power Electronics*, vol: 2, pp. 192-202, 2009.

[22] S. Sirisukprasert, "The Modelling and Control of a Cascaded-Multilevel Converter-Based STATCOM", PhD. Thesis, *Dept. ECE Virginia Tech.*, USA, 2004.

[23] N. Voraphonpiout, T. Bunyagul and S. Chatratana, "Analysis and Performance Investigation of a Cascaded Multilevel STATCOM for Power System Voltage Regulation*", International Energy Journal*, vol. 8, no. 2, 2007.

[24] P. Giroux, G. Sybille and H. Le-Huy, "Modeling and Simulation of a Distribution STATCOM using Simulink's Power System Blockset", *IECON'01: The 27th Annual Conference of the IEEE Industrial Electronics Society*, 2001, pp. 990-994.

[25] J. S. R. Jang, C. T. Sun and E. Mizutani, "Neuro-Fuzzy and Soft Computing", Prentice Hall, USA, 1997.

[26] M. Gökbulut, B. Dandil and C. Bal, "Development and Implementation of Fuzzy-Neural Network Controller for Brushless DC Motors", *Intelligent Automation and Soft Computing, An International Journal*, vol. 13, no. 4, pp. 423-435, 2007.

[27] M. Gökbulut, B. Dandil and C. Bal, "A Hybrid Neuro-Fuzzy Controller for Brushless DC Drives", *Lecture Notes in Artificial Intelligence*, vol: 3949, pp. 125-132, 2006.

[28] A. Cetin and M. Ermis, "VSC-Based D-STATCOM With Selective Harmonic Elimination", *IEEE Transactions on Industry Applications*, vol. 45 , pp. 1000 – 1015, 2009.